Published in final edited form as:
Prog Biophys Mol Biol. 2011 October ; 107(1): 48–59. doi:10.1016/j.pbiomolbio.2011.06.005.

Cardiac Myocytes and Local Signaling In Nano-Domains

Raimond L. Winslow and **Joseph L. Greenstein**
The Institute for Computational Medicine & Department of Biomedical Engineering, The Johns Hopkins University School of Medicine and Whiting School of Engineering, Baltimore, Maryland 21218 USA

Abstract

It is well known that calcium-induced calcium-release in cardiac myocytes takes place in spatially restricted regions known as dyads, where discrete patches of junctional sarcoplasmic reticulum tightly associate with the t-tubule membrane. The dimensions of a dyad are so small that it contains only a few Ca^{2+} ions at any given time. Ca^{2+} signaling in the dyad is therefore noisy, and dominated by the Brownian motion of Ca^{2+} ions in a potential field. Remarkably, from this complexity emerges the integrated behavior of the myocyte in which, under normal conditions, precise control of Ca^{2+} release and muscle contraction is maintained over the life of the cell. This is but one example of how signal processing within the cardiac myocyte and other cells often occurs in small "nano-domains" where proteins and protein-complexes interact at spatial dimensions on the order of ~ 1 – 10 nanometers and at time scales on the order of nanoseconds to perform the functions of the cell. In this article, we will review several examples of local signaling in nano-domains, how it contributes to the integrative behavior of the cardiac myocyte, and present computational methods for modeling signal processing within these domains across differing spatio-temporal scales.

Keywords

cardiac myocyte; excitation-contraction coupling; local signaling domain; multiscale modeling; computational modeling

1. Introduction

It is becoming increasingly clear that cellular signal processing often occurs in small "nano-domains", where proteins and protein-complexes interact at spatial dimensions ranging from 1's to 10's of nanometers, and on time scales of nanoseconds to microseconds. This mode of signaling in fact appears to be a common design motif in all cells, and is certainly true of the cardiac myocyte. In this article, we will present examples of the important role of such local signal processing in the cardiac myocyte. We will focus on the integration of Ca^{2+} and Na^{+} signals in and near the cardiac dyad.

Corresponding Author: Raimond L. Winslow, PhD, Hackerman Hall Rm 315, 3400 N. Charles Street, Baltimore MD 21218, USA, 410-516-5417 (Office), 410-516-5294 (FAX), rwinslow@jhu.edu.

Editors' Note
Please see also related communications in this issue by Cooper et al. (2011) and Katsnelson et al. (2011).

Calcium-induced calcium-release (CICR) in cardiac myocytes takes place within dyads, where discrete patches of junctional sarcoplasmic reticulum (jSR) tightly associate with the t-tubule membrane. Dyad volume, diameter, and height are estimated to be ~ 3×10^5 nm^3, 100 - 200 nm, and 10-15 nm, respectively (Franzini-Armstrong et al., 1999; Hayashi et al., 2009). L-type Ca^{2+} channels (LCCs) are preferentially located in the t-tubule membrane, in close apposition to the jSR membrane. As our initial example of signal processing in nano-domains, we will consider the remarkable, recent experimental and modeling evidence indicating that LCCs are able to sense both local Ca^{2+} concentration, as well as global Ca^{2+} signals. This signal processing results from the differing temporal dynamics of conformational changes due to Ca^{2+} binding to the C- versus N-lobe of calmodulin (CaM), which is tethered to LCCs and mediates Ca^{2+}-dependent inactivation. It is a compelling example of how an important regulatory signal can be sensed by a pair of molecules.

Because of the small physical dimensions of the dyad, modeling studies indicate that at any instant of time there are only a few (~ 1 - 100) Ca^{2+} ions present, and that Ca^{2+} signaling may be influenced significantly by the physical shape and size of the dyad, the relative placement of dyad proteins such as ryanodine receptors (RyRs) and LCCs, local membrane buffering of Ca^{2+} by negatively charged phospholipid headgroups, and the dyadic electric field. Our second case study will review how nano-scale models of Ca^{2+} signaling in the dyad that are based on the fundamental physical principles governing the trajectories of individual Ca^{2+} ions and their binding to RyRs, provide insights into the nature of dyadic Ca^{2+} signaling and CICR. Additional signal processing occurs in the dyad. Examples include signaling mediated by protein kinase A (PKA) and Ca^{2+}/CaM-dependent protein kinase II (CaMKII). These signaling molecules are part of complex macromolecular assemblies that help guide their phosphorylation of target proteins in the dyad. These signaling molecules also exert global whole-cell level actions. Our third case study will review computational models of the actions of these important signaling molecules.

Extra-dyadic processes operating at the length-scale of 10's to possibly 100's of nms are also likely to influence signal processing in the dyad by establishing "boundary conditions". Imaging studies have revealed that the Na^+-Ca^{2+} exchanger (NCX) is localized within and/or near the dyad, and experimental evidence suggests that Ca^{2+} entry via reverse-mode NCX activity may either trigger or modulate CICR. Recent evidence also indicates that the membrane adaptor protein ankyrin-B (ANK-B) binds to NCX, the Na^+-K^+ ATPase (NKA), and the inositol 1,4,5-phosphate operated Ca^{2+}-releasing channel ($InsP_3R$) in the T-tubules, creating the substrate for a macro-molecular signaling complex that may play a crucial role in modulating CICR and regulation of Na^+ and Ca^{2+} levels in the cardiac myocyte (Mohler et al., 2005). We will review experimental data regarding the functional role of extra-dyadic Na^+ and Ca^{2+} transporters and their possible organization into protein complexes, and suggest directions for future modeling of these systems.

Finally, as an additional example of extra-dyadic processes and their influence on dyad signal processing, we will consider the effects of close, physical approximation of mitochondria with the jSR. It is now known that mitochondria are localized within a few 10's of nms of, and are tethered to, the jSR. Mitochondria take up Ca^{2+} via the Ca^{2+} uniporter (mCU) and extrude Ca^{2+} through the mitochondrial Na^+-Ca^{2+} exchanger (mNCE). Recent data suggest that mCU transport in cardiac myocytes is fast, raising the possibility that positioning of mitochondria near the dyad may play a significant role in setting the boundary conditions regulating CICR and local Ca^{2+} transients on a beat-to-beat basis.

2. Signal Processing in the Cardiac Dyad

2.1 Sensing of Local and Global Ca^{2+} Signals by Calmodulin Molecules at the Site of the L-Type Ca^{2+} Channel

Ca^{2+} is a ubiquitous signaling molecule in the heart (as well as other organ systems) that plays a role in regulating a large variety of processes. In order to achieve coordinated signaling at the whole-cell level, cardiac myocytes must have mechanisms that allow for sorting of global and local Ca^{2+} signals in order to regulate processes such as gradation of contraction and heart rate (sensitive to global Ca^{2+}) as well as processes involved in energy production, transcription, and cell survival (sensitive to localized Ca^{2+}) (Anderson and Mohler, 2009). The cardiac dyad nano-domain is an example where a molecular Ca^{2+} sensor mediating Ca^{2+}-dependent inactivation (CDI) of the L-type Ca^{2+} current (I_{CaL}) is positioned in very close proximity to Ca^{2+} sources (LCCs and RyRs), allowing for privileged Ca^{2+} signaling. Recent studies (Dick et al., 2008; Tadross et al., 2008) have shed new light on the function of calmodulin (CaM) as a sensor for CDI of I_{CaL}, demonstrating the remarkable processing of the Ca^{2+} signal that can be performed by individual molecules within the dyad in order to sense local versus global Ca^{2+}.

Tadross et al (2008) used a combination of elegant models and experiments to elucidate the mechanisms underlying Ca^{2+} channel CDI, by which CaM can sense and decode local and global Ca^{2+} signals. CaM continuously complexes with LCCs and serves as the cytosolic Ca^{2+} sensor for CDI (Erickson et al., 2001). CaM is a bi-lobed protein, where both the N- and C-lobes bind Ca^{2+}, but with different affinities. Despite the fact that both lobes are in very close proximity to the LCC Ca^{2+} flux (i.e. ~10 nm from the channel pore), each lobe responds selectively to either the local (brief high-amplitude spikes in $[Ca^{2+}]$) or global (a longer lasting pedestal of $[Ca^{2+}]$) component of the Ca^{2+} signal. The ability of the LCC to respond selectively to either of these Ca^{2+} signals was explained by interpretation of a variety of experiments using the model shown in Figure 1. This model shows the states for the association of a single lobe of CaM with a Ca^{2+} channel. Transitions from state 1 through 4 represent dissociation of apoCaM from the Ca^{2+} channel, binding of 2 Ca^{2+} ions to a lobe of CaM, and binding of Ca^{2+}/CaM to the effector site for CDI. If the transitions between states 2 and 3 are slow relative to channel gating, then brief high-amplitude spikes in Ca^{2+} arising from channel gating will be sufficient to cause accumulation of channels in state 3, and subsequent transition to state 4 (CDI). This is the hypothesized mechanism for local Ca^{2+} sensing by the C-lobe of CaM. However, if the transition between states 3 and 2 is fast relative to the Ca^{2+} fluctuations associated with channel gating (in conjunction with slow transitions between states 1 and 2, and states 3 and 4), then global selectivity emerges (see Tadross et al (2008) for details). This yields a mechanism that is sensitive to fractional presence of Ca^{2+} over time (i.e. highly sensitive to weak but sustained Ca^{2+} signals), but insensitive to the intensity of the Ca^{2+} signal, and can explain N-lobe sensitivity. Furthermore, N-lobe selectivity can be switched between global and local properties by altering the function of an additional Ca^{2+}/CaM binding site on the N-lobe called NSCaTE (that normally restricts CaM to respond to local Ca^{2+} in Cav1 channels) (Dick et al., 2008). This mechanism for the selective molecular sensing of local versus global Ca^{2+} signals is without question remarkable. The implications of this selective Ca^{2+}-sensing mechanism on our understanding of dyadic Ca^{2+} dynamics and cardiac excitation contraction coupling (ECC) have yet to be studied within the context of models of the cardiac myocyte.

2.2 Mechanisms of Ca^{2+}-Induced Ca^{2+} Release in the Cardiac Dyad Nano-domain

LCCs and RyRs reside in close apposition on opposite sides of the dyadic cleft, effectively granting Ca^{2+} ions permeating an LCC privileged access to the Ca^{2+} binding sites on nearby RyRs. Importantly, the assumed structural separation of individual clefts (Franzini-

Armstrong et al., 1999) suggests that released Ca^{2+} does not generally act as a trigger to RyRs in distant dyads (though recent studies suggest neighboring RyR clusters may have a functional role in ECC (Baddeley et al., 2009; Rovetti et al., 2010)). Stern's landmark "calcium-synapse" model (Stern, 1992), in which each dyad was assumed to contain a single LCC and a single SR release channel, captured these ideas in an elegantly simple way, demonstrating that high gain and graded SR release arise from the local correlation in stochastic LCC and RyR gating due to their communication via a common local Ca^{2+} signal. This has become known as the local control theory of ECC. This idea is crucial in understanding how the microscopic properties of CICR translate into macroscopic physiologic phenomena observed in experiments. Graded Ca^{2+} release (as measured at the whole-cell level) is achieved in this model by statistical recruitment of elementary SR Ca^{2+} release events. This fundamental idea of local control of SR release has spurred a number of modeling studies, some of which are described below.

Due to the small size of the dyad, it became clear that understanding the spatial and temporal profile of dyadic Ca^{2+} concentration ($[Ca^{2+}]_d$) would be an important step in elucidating the mechanistic details of local CICR. Langer and Peskoff (1996) developed one of the first detailed models to numerically simulate the time course of dyadic Ca^{2+}. The model predicted that a single typical LCC opening led to ~ 1 mM $[Ca^{2+}]_d$ near the mouth of the LCC. The presence of sarcolemmal buffering sites slowed the decay of the local Ca^{2+} transient (such that it remained highly elevated long after LCC closure) as compared to the dynamics in the absence of buffers, a finding which was inconsistent with the idea that LCC gating imposes tight control on RyR activity. Soeller and Cannell (1997) formulated a dyad model which introduced the electrostatic effects of ion movement, and predicted that $[Ca^{2+}]_d$ actually changes more rapidly in response to LCC gating. In this model, $[Ca^{2+}]_d$ was approximately proportional to unitary LCC currents over a wide range of current amplitudes. The model yielded predictions of $[Ca^{2+}]_d$ profiles during jSR release which peaked as high as 300 μM near the center of the dyad. The decay in dyadic Ca^{2+} occurred in ~ 2 ms following termination of SR release (but this was sensitive to the dyad boundary condition). The high speed of the response of dyadic Ca^{2+} to LCC and RyR gating in this model helped to explain how tight local control of SR release by LCCs can be achieved.

CICR occurs in the form of discrete Ca^{2+} trigger and release events that underlie the observation of Ca^{2+} sparks. These events arise as a result of the interaction of a small number of channel proteins that interact within the domain of a single cardiac dyad. The small size of the dyadic cleft (~ 4×10^5 nm^3 with ~ 10 - 40 RyRs) (Baddeley et al., 2009; Hayashi et al., 2009), in combination with the relatively large proteins that reside in the cleft, results in a space in which Ca^{2+} diffusion is highly restricted. Figure 2 shows a representation of an LCC, RyR, and a single CaM molecule tethered to the LCC in the dyad based directly on structural data (Serysheva et al., 2005; Wang et al., 2004a; Wilson and Brunger, 2000). Models predict that during an AP, peak Ca^{2+} concentration in the dyad ranges from 100 to 1000 μM (Langer and Peskoff, 1996; Soeller and Cannell, 1997), which corresponds to as few as 20-200 free Ca^{2+} ions (Tanskanen et al., 2007). Thus, it is clear that both feed forward and feedback signaling between RyRs and LCCs in the dyad is likely mediated by relatively few Ca^{2+} ions. Therefore, application of laws of mass-action to analysis of signaling events mediated by this relatively small number of ions may not be appropriate (Bhalla, 2004). The stochastic motion of Ca^{2+} ions in the dyad may also impart a significant amount of signaling noise between LCCs and RyRs, thereby influencing the fundamental properties of CICR (Tanskanen et al., 2007). In addition, the physical location and dimensions of dyad proteins may play a considerable role on the nature of Ca^{2+} ion motion and hence, CICR.

To explore these issues, we recently developed a computational model of Ca^{2+} signaling in the dyad that simulates motion of Ca^{2+} ions, binding of ions to RyR receptor sites, and Ca^{2+} release from RyR. This model was developed in order to understand factors, such as those listed above, that determine properties of CICR at the level of the cardiac dyad. We addressed the following three questions: 1) what is the number of Ca^{2+} ions that are present in the dyad during CICR?; 2) how does the physical arrangement of large proteins within the dyad influence CICR?; and 3) how does "signaling noise" due to the potentially small number of Ca^{2+} ions within the dyad affect the nature of CICR? We addressed these questions by developing a molecularly- and structurally-detailed computational model of the cardiac dyad describing motions of Ca^{2+} ions, as influenced by thermal energy and electrostatic potentials.

Development of the nano-scale model is presented in detail elsewhere (Tanskanen et al., 2007). Briefly, a simplified dyad was modeled using a 200 nm × 200 nm × 15 nm lattice containing 20 RyRs arranged in a 4 × 5 matrix. Four LCCs were positioned randomly across this lattice to achieve a 5:1 RyR:LCC ratio. The geometry of each LCC and RyR protein was modeled as shown in Fig. 2, with each LCC tethering one CaM. The geometry of the Ca^{2+}-accessible dyadic volume was determined by the presence, shape, and location of these proteins, which due to their large size relative to the dyad occupy a significant fraction of the dyadic volume. LCCs and RyRs were modeled using continuous-time, discrete-state Markov processes. LCC gating was simulated stochastically using a previously developed Markov model of the LCC (Greenstein and Winslow, 2002; Jafri et al., 1998) in which Ca^{2+} binding induced a shift in LCC gating dynamics into a low open probability mode representative of CDI. The LCC model incorporated a separate mechanism for voltage-dependent inactivation (VDI) as well. The gating kinetics of the RyR were described using the four-state Markov model of Stern (Stern et al., 1999; Wang et al., 2004b). CDI of an LCC required that the two C-lobe Ca^{2+} binding sites of the associated CaM were occupied. Opening of RyR required that Ca^{2+} was bound to all four activation sites. RyRs were assumed to inactivate when Ca^{2+} was bound to at least one out of four distinct inactivation sites. See Tanskanen et al. (2007) for a detailed description of how the locations of the activation and inactivation Ca^{2+}-binding sites were determined. In this model, Ca^{2+} binding to the channel protein must be considered separately from the subsequent conformational change of the channel protein (steps that are typically combined in most channel models). It was assumed that a Ca^{2+}-dependent state transition requires that Ca^{2+}-binding sites are first occupied by Ca^{2+} ions. When a freely diffusing Ca^{2+} ion enters a lattice position adjacent to an available Ca^{2+}-binding site, that Ca^{2+} ion has the opportunity to bind to the site. The relative magnitude of the binding rate compared to the rate of diffusion determines the probability that the Ca^{2+} ion either binds to the site or diffuses away. Ca^{2+}-binding transitions were incorporated into the overall model of Ca^{2+} movement in the dyad (see below). Ion channel transition rates were therefore defined as functions that depend upon the occupancy of the Ca^{2+} binding sites (rather than $[Ca^{2+}]_d$). Entry of Ca^{2+} ions into the dyad via open LCCs and RyRs was modeled as a Poisson process with rate governed by channel permeabilities measured experimentally (Rose et al., 1992). Sarcolemmal anionic sites acted as Ca^{2+} buffers and site density and Ca^{2+} binding/unbinding rates were based on the work of Langer and Peskoff (1996) and Soeller and Cannell (1997). The joint positions of Ca^{2+} ions present in the dyad were assumed to behave as Brownian motion in a potential field, where Ca^{2+} ion could interact with other Ca^{2+} ions as well as electrostatic potentials. The time-evolution of Ca^{2+} ions were therefore well described by the Fokker-Planck equation (FPE) (Risken, 1997) and we modeled the joint positions of N Ca^{2+} ions present in the dyad as a $3N$-dimensional Brownian motion in a potential field, as described by the FPE. The total potential energy of the system (given as a function of Ca^{2+} ion positions) was determined within the FPE based on the assumptions that: (1) an electrostatic potential forms at each ion due to the charges on the surrounding proteins and lipids, (2) proteins within the dyad are impenetrable by Ca^{2+}

ions, and (3) the Debye length for Ca^{2+} ions in the dyad is ~ 1 nm which means that two Ca^{2+} ions cannot occupy the same lattice point at the same time but otherwise have no electrostatic interaction (i.e. at distances greater than 1 nm). The lateral boundary at the interface between the dyadic volume and myoplasm was treated as an absorbing boundary for ions flowing from the dyad to the myoplasm. The multidimensional FPE describes the evolution of the probability density function for the positions of Brownian particles subject to a potential. Rather than solving the time-dependent joint probability density from the FPE, we generated the net evolution of Ca^{2+} ion positions in the dyad using an algorithm for a finite difference representation of the FPE that can be interpreted as a spatially discrete Markov process as described by Wang et al (2003) and simulated using Monte Carlo methods. The discrete description of Ca^{2+} dynamics in the dyad was coupled with the processes of Ca^{2+} binding and gating dynamics of RyRs and LCCs. The incorporation of these processes allowed the entire dyad to be simulated by a single all-inclusive Markov process (Tanskanen et al., 2007).

The peak number of free Ca^{2+} ions in the dyad has previously been estimated to be small, ~ 1 free Ca^{2+} ion at a Ca^{2+} concentration of 10 μM in a dyad of radius 50 nm (Bers, 2001). A 10-ms simulation of a model dyad containing only one LCC located at its center at a membrane potential of 0 mV generated an average of ~ 0.5 Ca^{2+} ions within a 50 nm radius of the LCC (see Fig. 8 of (Tanskanen et al., 2007)), with a minimum of zero and a maximum of 7 Ca^{2+} ions (corresponding to a maximum concentration of 98.7 μmol/L $[Ca^{2+}]_d$). A similar protocol using a single RyR in the SR membrane (in which the RyR is initially open) generated an average of ~ 22.8 Ca^{2+} ions. The number of Ca^{2+} ions peaked at 49 during Ca^{2+} release, which corresponds to a concentration of ~ 0.7 mmol/L Ca^{2+}, similar to jSR Ca^{2+} concentration (Shannon et al., 2000). RyR gating produced a high degree of variability in the number of dyadic Ca^{2+} ions (coefficient of variation of 64%), showing that the LCC-RyR signaling involved in CICR at the level of the single dyad is a noisy process mediated by tens of Ca^{2+} ions.

Features of a representative single dyad Ca^{2+} release event are shown in panels A and B of Fig. 3. Ca^{2+} release is evoked by a voltage clamp to 0 mV at time zero. Panel A shows the number of Ca^{2+} ions in the dyad, and panel B shows the number of LCCs (gray line) and RyRs (black line) that are open as a function of time during the release event. Two LCCs open at ~ 3 ms following the voltage clamp, and Ca^{2+} influx into the dyad triggers the opening of 3 RyRs 1-2 ms later, which inactivate after ~ 7 ms, ~ 9 ms, and ~ 13 ms, respectively. The temporal shape of the Ca^{2+} signal in the dyad (Fig. 3A) is closely correlated to the number of open RyRs (Fig. 3B). Figure 3C shows the average number of Ca^{2+} ions in the dyad based on the simulation of 1000 independent dyads. As would be expected the peak of the average signal is reduced compared to that of an individual dyad due to temporal dispersion of Ca^{2+} release events and the fact that not all dyads will exhibit a Ca^{2+} release event. The duration of the average local Ca^{2+} transient shown in Panel C is ~ 20 ms (at half-maximal amplitude), similar to that measured for Ca^{2+} spikes in myocytes (Cheng et al., 1993; Sham et al., 1998; Song et al., 2001).

Despite the noisy nature of dyad signaling, simulations showed that ECC gain is a robust and reproducible feature that emerges from the underlying assumptions of the model made at the nano-scale level. For a whole-cell population of dyads, the variability in gain that arises from the stochastic gating of LCCs and RyRs is small at potentials near and above 0 mV (see Fig. 11 of (Tanskanen et al., 2007)). The functional influence of protein structures on ECC is shown in Fig. 3D. Peak ECC gain (measured as the average over 400 independent dyad simulations) obtained for the baseline model (solid line) is compared to that for the model in which LCC, RyR, and CaM molecule structures were omitted (dashed line). Ca^{2+} binding site locations were the same for both simulations. Over a wide range of potentials,

the peak ECC gain is decreased upon removal of the protein structures from the dyad. The protein structures occupy ~ 15% of the dyad volume. In order to show that the difference in ECC gain in the presence vs. absence of protein structures is not simply attributable to the difference in Ca^{2+}-accessible dyad volume, peak ECC gain was obtained with protein structures absent and dyad volume reduced by ~ 15% (dotted line). ECC gain values for this model were clearly not increased to the level obtained in the presence of protein structures. These data indicate that the physical shape and configuration of dyad proteins influences Ca^{2+} diffusion during CICR in such a way as to enhance ECC gain. In addition, the probability of triggering a release event with protein structures intact (0.152) was 44% greater than with protein structures excluded (0.105). These data suggest that when LCCs are directly apposed to RyRs, the diffusion obstacle imposed by the structure of RyRs leads to an increase in the probability that trigger Ca^{2+} ions bind to activation sites on the RyRs, and hence increases ECC gain.

These data demonstrate that a number of features of CICR arise from mechanisms underlying the interaction of LCCs and RyRs at the level of single dyads: 1) CICR is a highly noisy process and that models based on laws of mass action may not accurately capture dyadic Ca^{2+} dynamics; 2) in ensembles of dyads, the fundamental properties of local control of CICR arise *de novo* as a consequence of the underlying physical structure and channel gating properties, including voltage-dependence of ECC gain; and 3) the physical shape and location of RyRs relative to LCCs is likely to have a major influence on properties of CICR.

2.3 CaMKII-dependent Modulation of Excitation-Contraction Coupling

An important Ca^{2+} cycling regulatory mechanism of recent interest is the signaling pathway involving Ca^{2+}/CaM-dependent protein kinase II (CaMKII), which targets and phosphorylates LCCs and RyRs in the cardiac dyad. In addition, CaMKII targets the network sarcoplasmic reticulum (nSR) Ca^{2+}-ATPase known as the SERCA pump, and phospholamban (PLB, a regulator of the SERCA pump). CaMKII also targets Na^+ and K^+ channels in the sarcolemma (Maier and Bers, 2007). Phosphorylation of these target proteins has multiple functional consequences. CaMKII plays a role in fine tuning ECC, and is activated when bound by Ca^{2+}/CaM. Evidence suggests that CaMKII is directly associated with its target proteins (Currie et al., 2004; Hudmon et al., 2005), indicating that CaMKII signaling occurs locally in the dyadic junction. In addition, CaMKII activity is elevated in heart failure (Ai et al., 2005). Saucerman and Bers (2008) incorporated models of CaM, CaMKII, and calcineurin (CaN) into the Shannon et al (2004) model of the cardiac myocyte in order to better understand the functional consequences of the different affinities of CaM for CaMKII and CaN during action potentials (APs). The model predicted that in the cardiac dyad, Ca^{2+} levels lead to a high degree of CaM activity resulting in frequency-dependent CaMKII activation and constitutive CaN activation, whereas the lower Ca^{2+} levels in the cytosol only minimally activate CaM, which allows for gradual CaN activation, but no significant activation of CaMKII. Grandi et al (2007) developed a model of CaMKII over-expression in rabbit ventricular myocytes, including the role of CaMKII phosphorylation of fast Na^+ channels, LCCs, and the transient outward K^+ current (I_{to1}), which revealed a net effect of action potential duration (APD) reduction with CaMKII.

Recently, Hashambhoy et al (2009) described dynamic CaMKII phosphorylation of LCCs in an extension of the Greenstein-Winslow (Greenstein and Winslow, 2002) cardiac myocyte model. In this model, it is assumed that a single CaMKII holoenzyme is tethered to each LCC, each CaMKII monomer can transition among a variety of activity states (see Fig. 2 of Hashambhoy et al (2009)), and CaMKII monomers can catalyze phosphorylation of individual LCCs. It is a biochemically detailed, stochastic model in which the activity state of each of 12 CaMKII monomers within a CaMKII holoenzyme and the phosphorylation

state of each LCC are simulated dynamically in addition to LCC voltage- and Ca^{2+}-dependent gating. In this model, active CaMKII monomers can phosphorylate neighboring CaMKII monomers and/or the associated LCC. These studies demonstrated that CaMKII-dependent shifts of LCC gating patterns into high activity gating modes (where phosphorylated LCCs experience openings that are 10-20 times longer in duration than non-phosphorylated LCCs) may be the key mechanism underlying experimentally observed increases of I_{CaL} amplitude (Fig. 4A), the apparent macroscopic increase in the rate of recovery from inactivation, and the slowing of inactivation rate associated with I_{CaL} facilitation. Hashambhoy et al (2010) further expanded this model to include CaMKII-dependent regulation of RyRs in the dyad and demonstrated that under physiological conditions, CaMKII phosphorylation of LCCs ultimately has a greater effect on RyR leak flux and APD as compared with phosphorylation of RyRs (Fig. 4B). The LCC phosphorylation mediated increase in diastolic RyR leak was attributed to the augmented cytosolic (and dyadic) Ca^{2+} level resulting from increased Ca^{2+} influx via LCCs under conditions that promote high LCC activity, and hence, high open probability. APD was shown to correlate well with a CaMKII-mediated shift in modal gating of LCCs (Fig. 4C).

2.4 Localized Signaling in the β-adrenergic Pathway

Cardiac ion channels as well as proteins involved in CICR and ECC are primary targets for regulation via the β-adrenergic signaling cascade. The so-called “fight or flight” response increases cardiac contractility and output via the release of neurotransmitters and hormones by the sympathetic nervous system. Norepinephrine and epinephrine bind to β-adrenergic receptors (β-ARs) on the myocyte surface. These are G-protein-coupled receptors which trigger the activation of adenylyl cyclase (AC), leading to the production of cyclic AMP (cAMP), which in turn activates protein kinase A (PKA). The numerous targets of PKA-mediated phosphorylation include LCCs and RyRs in the cardiac dyad, PLB in the nSR, the myofilament protein troponin I, and phospholemmen (a subunit of the Na^+-K^+ pump) (Bers, 2002; Bers, 2008; El-Armouche and Eschenhagen, 2009). Recent studies have revealed that cAMP signaling does not occur within a simple linear pathway, and this has led to the hypothesis of cAMP compartmentation, in which the cell maintains distinct localized domains of cAMP (Saucerman and McCulloch, 2006). A possible mechanisms for cAMP compartmentation is the existence of caveolae, membrane invaginations in which high concentrations of β-adrenergic signaling proteins such as β-ARs, ACs, and PKA have been found in cardiomyocytes (Ostrom et al., 2001). In addition, LCCs (a major PKA target) have been found to co-localize with caveolae (Lohn et al., 2000). A-kinase-anchoring proteins (AKAPs) may also play an important role in the compartmentalization of β-adrenergic signaling by tethering PKA near its targets. In the heart it has been shown that AKAPs target PKA to LCCs, RyRs, type 2 β-ARs, as well as mitochondria and other sites (Ruehr et al., 2004; Saucerman and McCulloch, 2006).

Early attempts to model the effects of PKA-mediated phosphorylation of its targets on the properties of CICR and the AP involved modeling the stimulated cell by altering the function of the target proteins based on the measured effects of phosphorylation. Greenstein et al (2004) developed a model of the canine ventricular myocyte in the presence of 1 μM isoproterenol (a β-AR agonist). This model could explain PKA-mediated changes in AP shape, dissected the specific effects of PKA-mediated phosphorylation of LCCs and RyRs on the voltage-dependent gain of CICR, and predicted a mechanism by which increasing levels of LCC phosphorylation could lead to increased frequency of early after depolarizations (Tanskanen et al., 2005). However, this model did not describe the dynamics of the β-adrenergic signaling pathway. Saucerman et al (2003) developed a differential-algebraic kinetic model of the β-adrenergic signaling pathway, and incorporated it into the rabbit myocyte model of Puglisi et al (2001). This model comprehensively describes the full

pathway including agonist stimulation of the type 1 β-AR, activation of G_s protein, cAMP synthesis by AC, cAMP degradation by phosphodiesterase, PKA subunit activation and dissociation, phosphorylation of important target proteins PLB and LCCs, and β-AR kinase and PKA-mediated type 1 β-AR desensitization. Mobile and anchored forms of PKA and protein phosphatases were accounted for separately. A wide range of independent biochemical and physiological experimental data was used to validate the model, strengthening its ability to make mechanistic predictions, and establishing it as a core signaling model upon which others would build in future studies. This model was used to understand effects of specific molecular perturbations (e.g. expression changes in AC and β-AR density) on cAMP dynamics and contractility via changes in function of target proteins resulting from altered phosphorylation dynamics. Recently, the model of Saucerman et al (2003) was incorporated into the guinea pig ventricular model of Faber and Rudy (2000) in a study of the role of β-adrenergic agonists and antagonists in long-QT syndrome (Ahrens-Nicklas et al., 2009). The model of Saucerman et al (2003) has also been adapted in order to investigate the role of β-adrenergic signaling on Na^+ regulation during EC coupling (Kuzumoto et al., 2008), and it was demonstrated that phospholemman has an important role in limiting the build-up of Na^+ during β-adrenergic stimulation, a finding that was later validated experimentally (Bers and Despa, 2009; Despa et al., 2008).

Integration of signaling models of the β-adrenergic pathway with experimental techniques has recently enabled more detailed studies of cell signaling kinetics and localization. Saucerman et al (2006) combined a spatially explicit version of their model (Saucerman et al., 2003) with FRET imaging experiments to show how spatial PKA gradients could be explained by restricted diffusion of cAMP, phosphodiesterase-mediated cAMP degredation, or PKA-mediated cAMP buffering, and concluded that cAMP compartmentation likely plays an important role in limiting the rate of PKA activation (Yang and Saucerman, 2011). An approach combining mathematical modeling with FRET experiments was also used by Iancu et al (2007), in which it was demonstrated that subcellular localization of different AC isoforms (which can be either stimulated or inhibited by the G_i G-protein) can explain the mechanism by which both stimulatory and inhibitory responses in cAMP can arise in response to the same upstream stimulus (acetylcholine-mediated activation of the muscarinic M_2 receptor). While there is still much that remains unknown regarding the mechanisms underlying localization of key proteins in the β-adrenergic signaling pathway, new approaches such as this will continue to elucidate the key mechanisms for localization and regulation of this cell signaling pathway.

2.5 The Function of Extra-Dyadic Localization of Ca^{2+} and Na^+ Channels and Transporters

Following CICR in cardiac myocytes, Ca^{2+} entering the cytosol must be removed in order to allow for mechanical relaxation and refilling of the heart. In steady state, it must be true that on each beat, Ca^{2+} that has been released from the SR via RyRs is pumped back into the SR, and Ca^{2+} that has entered the cell via LCCs is extruded from the cell. The dominant Ca^{2+} efflux mechanism in cardiac myocytes is NCX. While the primary function of NCX is to remove Ca^{2+} from the myocyte during diastole, numerous studies have indicated that NCX can operate in a so-called reverse mode in which Ca^{2+} is imported and Na^+ is extruded, potentially providing an alternative source of Ca^{2+} influx during CICR. Given that CICR occurs in the form of discrete Ca^{2+} sparks within the dyad, functional evidence for a role of NCX in triggering SR Ca^{2+} release would suggest that NCX must be located within or near the dyad, and therefore may participate in the Ca^{2+} signaling events that occur in this nano-domain. Whether or not Ca^{2+} entry via reverse mode NCX contributes to the trigger for CICR remains controversial, as there are data that argue both for and against this mechanism. Bouchard et al (1993) measured the voltage dependence of cell shortening in rat ventricular myocytes and observed no significant effect of altering the electrochemical

gradient for Na^+ (which would alter NCX function). In addition, rapid phasic contractions were never elicited under conditions where LCC Ca^{2+} influx was blocked, suggesting NCX alone could not trigger CICR. Sham et al (1992) saw no evidence that Na^+ influx (via fast Na^+ channels) or its accumulation could initiate SR Ca^{2+} release. Sipido et al (1997) analyzed the characteristics of SR Ca^{2+} release triggered by reverse NCX and I_{CaL} in isolated guinea pig ventricular myocytes, and found that trigger efficiency for reverse mode NCX was about four times less than that for I_{CaL}. Moreover, they could detect no contribution of reverse mode NCX to the CICR trigger at potentials below 60 mV when I_{CaL} was intact, suggesting that the role of NCX in triggering CICR during the cardiac AP was negligible. In contrast to these studies, Litwin et al (1998) found that reverse mode NCX alone could not provide enough Ca^{2+} influx to activate myofilaments directly, but that the nifedipine-insensitive current carried by NCX could trigger a component of contraction that increased with voltage, suggesting reverse NCX can trigger SR Ca^{2+} release. Similarly in rat ventricular myocytes at near physiological conditions, Wasserstrom et al (1996) found that under both voltage- and AP-clamp protocols, about 50% of the elicited contraction was nifedipine-insensitive, and that this component of contraction could be blocked by Ni^{2+} (which blocks NCX), suggesting that reverse mode NCX contributes to CICR.

More recent experiments have attempted to address the controversial role of NCX in triggering SR Ca^{2+} release. Sobie et al (2008) imaged the trigger flux of Ca^{2+} across the cell membrane using a fluorescent Ca^{2+} indicator under conditions where Ca^{2+} release from the SR was disabled and found a significant contribution of reverse mode NCX to the total Ca^{2+} influx. However, NCX-mediated Ca^{2+} entry was found to be considerably smaller when measured in the absence of I_{CaL}, suggesting that the local elevation of $[Ca^{2+}]$ that occurs upon LCC activation is necessary to activate nearby NCX via a catalytic Ca^{2+}-binding site (Hilgemann et al., 1992). Lack of NCX catalysis may explain the observation that NCX plays no role in triggering CICR in earlier studies. Neco et al (2010) have examined Ca^{2+} sparks in wild-type (WT) and cardiac specific NCX knock-out (KO) mice, and found that high sub-sarcolemmal Ca^{2+} must be maintained in KO mice for synchronous triggering of Ca^{2+} sparks resembling those of WT. In WT, NCX could prime the dyad with sufficient Ca^{2+} for normal spark triggering (so intervention to raise sub-sarcolemmal Ca^{2+} was not necessary), suggesting that the ability to generate normal Ca^{2+} sparks depends upon the presence of nearby NCX. Furthermore, Larbig et al (2010) showed that Ca^{2+} transients and SR Ca^{2+} release flux of KO mice were unaffected by inactivation (or block) of I_{Na} whereas those of WT were reduced by ~ 50%, and concluded that I_{Na}, via its effect on reverse mode NCX, modulates Ca^{2+} release in WT myocytes by enhancing the Ca^{2+} signal in the vicinity of the RyRs during CICR.

In agreement with these functional data, imaging studies indicate that up to 50-70% of NCX are located within t-tubules (Scriven et al., 2000; Thomas et al., 2003; Yang et al., 2002), and this localization is mediated by NCX binding to the membrane adaptor protein ankyrin-B (ANK-B) (Cunha et al., 2007) at ANK repeats 16 – 18 (Cunha and Mohler, 2009). As described above, the spatial distribution of NCX expression in the t-tubules, and in particular location relative to RyRs, has been a subject of great interest because of its implications for ECC processes. Using fluorescently tagged antibodies to both RyRs and NCX, Scriven et al (2000) observed virtually no co-localization of expression, suggesting that NCX is positioned in the extra-dyadic region of the t-tubules (Scriven et al., 2000). More recently, Jayasinghe et al (2009) used improved imaging techniques to show that NCX labeling in t-tubules has an approximately uniform distribution that is interrupted by local regions of more intense labeling, referred to as puncta. Many of these puncta are very close to RyR clusters, with mean distance to the nearest cluster being ~ 250 nm. If correct, these data show that NCX is not only localized in t-tubules, but may be sufficiently close to the dyad to have a significant effect on ECC.

Cardiac myocytes also express both α1 and α2 isoforms of the Na^+-K^+ ATPase (NKA). The α2 isoform (NKA-α2) is known to be expressed preferentially in the t-tubules (Swift et al., 2007). ANK-B binds directly to the N-terminal tail of the catalytic α-subunit of NKA (Liu et al., 2008), and both NKA-α1 and NKA-α2 expression in t-tubules is markedly reduced in haplo-insufficient ANK-$B^{+/-}$ myocytes. Thus, as with NCX, ANK-B mediates localization of NKA in the t-tubule region. The fact that both NCX and NKA-α2 may require ANK-B for stable expression raises the possibility that NCX1 and NKA-α2 are co-localized in the t-tubules. This appears to be the case in several cell types. In cultured astrocytes, NKA-α2 and NCX expression is co-localized to a micro-domain between the plasma and endoplasmic reticulum (ER) membrane (Golovina et al., 2003). NKA and NCX are also co-localized in the inner segment of rod photoreceptors, and this co-localization is dependent on expression of ANK-B (Kizhatil et al., 2009). In cardiac myocytes, ANK-B co-immunoprecipitates with NCX1, NKA-α1/α2, and $InsP_3Rs$ (Mohler et al., 2003). ANK-B is necessary for this co-localization (Mohler et al., 2005). Consistent with these data, ANK-B is known to have a binding site for $InsP_3R$ that is distinct from those for NCX and NKA (Kline et al., 2008).

Based on these findings, Ackerman and Mohler (2010) have proposed the structural model shown in Fig. 5 of ANK-B complex formation within t-tubules (Mohler and Wehrens, 2007). This figure shows interactions between ANK-B, actin associated β2-spectrin, the cytoskeletal protein obscurin, as well as NCX, NKA, and $InsP_3R$. The three distinct binding sites of an ANK-B molecule are capable of binding one molecule each of NKA, NCX, and $InsP_3R$, configuring them into a local complex interacting over a distance of 10-20 nm. It is also possible that ANK-B can bind one or two of these molecules at a time. This raises many possibilities for local Na^+ and Ca^{2+} signal integration. In the case of a local complex comprised of an NCX and NKA molecule bound to ANK-B, Na^+ extrusion via NKA may quickly deplete local Na^+ concentration, facilitating transport of Ca^{2+} out of the t-tubules via NCX, whereas inhibition of NKA, through local increase of Na^+, may facilitate reverse mode NCX function. This close coupling of NKA and NCX activity is consistent with the observations of Terracciano (2001) and Su et al (2001) in experiments where NKA activity was rapidly inhibited, producing significantly decreased NCX-driven Ca^{2+} extrusion and increased Ca^{2+} transients, similar to the effects of oubain on NKA and SR Ca^{2+} load. The functional significance of a local complex comprised of NKA, NCX, and $InsP_3R$ is much less clear. One hypothesis is that when this complex is localized to the extra-dyadic region of the t-tubules, $InsP_3Rs$ can modulate CICR. $InsP_3R$ activation may enhance the likelihood of Ca^{2+} sparks and waves through regulation of local Ca^{2+} levels. Functionally, an E1425G mutation in ankyrin-B causing dominantly inherited type 4 long-QT cardiac arrhythmia in humans leads to loss of ANK-B-associated NCX, NKA, and $InsP_3R$, and results in defects of intracellular Na^+ and Ca^{2+} regulation and cellular after-depolarizations in response to catecholamines (Mohler et al., 2003). The mechanisms of such complex interactions will only be resolved through development of computational models that capture the ability of these protein complexes to integrate local Na^+ and Ca^{2+} signals.

2.6 The Mitochondrial - JSR Local Ca Signaling Domain

Even at resting heart rates, the process of ECC consumes significant amounts of ATP. The main consumers are the myosin ATPase, NKA, and the SERCA pump. Estimates suggest that at maximal workload, the entire cellular ATP pool may be utilized over a time-course of a few seconds (Balaban, 2002). Maintaining the process of ECC therefore requires that mitochondrial ATP production be tightly controlled by myocyte workload, potentially on a beat-to-beat basis. It is therefore no wonder that understanding the mechanisms by which control is exerted has been a central theme of cardiac biology over the last several decades.

The early work of Chance and Williams indicated that energy supply and demand matching is regulated by levels of ADP and P_i through effects on the F1/F0-ATPase (Chance and

Williams, 1955). This hypothesis was called into question when Balaban and colleagues (Territo et al., 2001) discovered that increased cardiac workload increased O_2 consumption without changes in the levels of ADP or P_i. This group went on to demonstrate that Ca^{2+} may play a major role in energy supply and demand matching by regulating activity of three enzymes in the tri-carboxcylate acid cycle (pyruvate, isocitrate, and a-ketoglutarate de-hydrogenase) and the F1/F0-ATPase, and that this regulation could be achieved on a time scale of ~ 100 msec (Territo et al., 2001).

In order for Ca^{2+} to be a regulator of energy supply-demand matching, sufficient Ca^{2+} must be transported into mitochondria to regulate TCA cycle enzymes and the F1/F0-ATPase. Ca^{2+} is transported into mitochondria by the mitochondrial Ca^{2+} uniporter (mCU). Careful modeling of the mCU (Dash et al., 2009) based on the experimental data of Scarpa and Graziotti (1973) shows that mCU transport rate is a sensitive function of extra-mitochondrial Ca^{2+} over the range of ~ 20 – 100 μM. These Ca^{2+} concentrations are much larger than observed in the cytosol, raising the question of how fluctuations of cytosolic Ca^{2+} can regulate ATP production. The answer may be due to the close proximity of mitochondria to the JSR and cardiac dyad. Using high-resolution optical imaging techniques, Rizutto et al (1998) showed that there appear to be numerous close contacts between mitochondria and endoplasmic reticulum in living HeLa cells. In addition, Ca^{2+} transients measured by targeting a Ca^{2+}-sensitive photo-protein to the outer face of the inner mitochondrial membrane, and then evoking Ca^{2+} release through $InsP_3R$ by application of histamine suggested that the mitochondrial surface was exposed to significantly higher Ca^{2+} concentration changes than observed in the cytosol. Subsequently, Csordas et al (2006) showed that rat liver mitochondria are connected with smooth and rough ER by structures they referred to as “tethers”. Tethers between the outer mitochondrial membrane (OMM) and smooth ER had lengths in the range of 9 – 16 nm, whereas those between OMM and rough ER had lengths 19 – 30 nm (Csordas et al., 2006). These data established a length-scale over which mitochondria and Ca^{2+} sequestering organelles may interact. In a recent elegant study, Hayashi et al (2009) showed the existence of similar electron-dense structures between the OMM and nSR/jSR in mouse ventricular myocytes, thus establishing the close proximity of cardiac mitochondria to the jSR membrane and Ca^{2+} release sites (Perkins et al., 2001) – a necessary component of the hypothesis that tight control of energy supply and demand in heart is regulated via mitochondrial sensing of local Ca^{2+} signals.

This hypothesis is also supported by predictions of local Ca^{2+} concentration in and near the cardiac dyad. Computational models predict that dyadic Ca^{2+} concentration may be as large as ~ 50 - 100 μM at the peak of the Ca^{2+} transient, and have rapid rise and decay times (< 10 ms) (Soeller and Cannell, 2004; Tanskanen et al., 2007). While these model estimates depend on many factors, they demonstrate that it is possible for the local Ca^{2+} signal near mitochondria to be large enough to activate mCU transport, and have sufficiently fast kinetics to support beat to beat regulation of mitochondrial energetics.

Tight regulation of mitochondrial energy production also requires that the mCU have sufficiently fast kinetics to respond to the local signal. Whether or not this is true remains controversial (Maack and O’rourke, 2007). Estimates of the time constant of mCU uptake differ, with some in the range of ~ 5 sec (Sedova et al., 2006), and others of ~100 ms (Territo et al., 2001). In addition, a recent study by Maack et al (2006) suggests that the mitochondrial Ca^{2+} transient always precedes the cytosolic Ca^{2+} transient, has faster mean rise time (15 ms versus 40 ms), and an average decay time of ~ 90 ms. Thus, while there remains controversy as to whether changes in mitochondrial Ca^{2+} are fast enough to follow each heart beat, there is increasing evidence that mitochondria sense Ca^{2+} in a local domain near the cardiac dyad, and that this sensing supports changes in mitochondrial Ca^{2+} over individual to 10’s of heart beats.

Implications for our understanding of both properties of ECC as well as control of mitochondrial energetics are significant. Furthermore, it is likely that mitochondria not only sense local Ca^{2+}, but also regulate local Ca^{2+} by virtue of their Ca^{2+} "buffering" (i.e., Ca^{2+} uptake via mCU) properties. Accordingly, co-location of mitochondria with jSR may have an important influence on properties of ECC by helping to set the boundary conditions on Ca^{2+} flux in the vicinity of cardiac dyads. Mitochondria may also effect Ca^{2+} communication between adjacent dyads, thereby influencing cellular properties such as conduction velocity of Ca^{2+} waves. Such effects may be particularly important in light of new evidence that the nearest neighbor distance between dyadic clefts may be as small as 20 nm (Hayashi et al., 2009). For all of these reasons, computational models that incorporate close interaction between mitochondria and the cardiac dyad, and sensing of the local dyadic Ca^{2+} signal, will be necessary in order to understand properties of beat to beat regulation of cardiac energetics, and local versus more global properties of Ca^{2+} signaling. The basis for modeling these processes has been established by development of compartmental models of ATP production in cardiac mitochondria (Beard, 2005; Cortassa et al., 2003) and integration of these mitochondrial models into models of the cardiac myocyte (Cortassa et al., 2006; Cortassa et al., 2009; Matsuoka et al., 2004a; Matsuoka et al., 2004b).

3. Conclusions

We have described a variety of biophysical processes relating to CICR that involve molecular interactions over nm length- and ns time-scales. It has become clear from both experimental and modeling studies that understanding nano-scale dyanamics, whether it is the processing of the dyadic Ca^{2+} signal by LCC-tethered CaM in the cardiac dyad, the interaction among LCCs and RyRs during CICR via a small number of Ca^{2+} ions, the mechanisms of local signaling in the CaMKII and β-adrenergic pathways, functional formation and consequences of local domains defined by colocalization of Ca^{2+} and Na^{+} transport mechanisms, or the local interaction of mitochondrial Ca^{2+} transport with CICR in the dyad, provides critically important insight into cellular function. Examples of similar nano-scale interactions abound in other cells (Golovina et al., 2003; Kizhatil et al., 2009; Modchang et al., 2010; Sosinsky et al., 2005). Understanding how integrative cellular, tissue, and whole organ function emerges from a variety of subcellular component mechanisms is the goal of multi-scale modeling techniques. Modeling such complex systems will require application of careful approximations that permit model integration across a range of time- and spatial-scales. In some cases, it has been possible to build self-contained multi-scale models of a physiological system. As an example, the model of Greenstein and Winslow (2002) spans the biological scales of single channel gating to whole cell physiology in a cardiac myocyte. In other cases, it is necessary to use the knowledge obtained from a detailed model at the nano-scale, e.g. mechanisms of ECC gain in the dyad (Tanskanen et al., 2007), to constrain models that are built at a more macroscopic scale, e.g. biophysically detailed whole cell models (Greenstein et al., 2006; Saucerman and McCulloch, 2006).

We are in the early days of multi-scale modeling, and a valuable approach to building a repertoire of methods for multi-scale approximations is to work example by example. In that spirit, we offer the work of Tanskanen and Winslow (2006) as a detailed example. The starting point of this work was the nano-scale model of the dyad (Tanskanen et al., 2007), presented in Sect. 2.2, describing the motion of individual Ca^{2+} ions at nm length- and ns time-scales based on the Fokker-Planck equation. To simplify the model, it was assumed that: (1) Ca^{2+} ions are independent and do not interact; (2) the entry of Ca^{2+} ions can be described as a continuous influx of probability mass; (3) Ca^{2+} buffering by mobile buffers does not affect the steady state Ca^{2+} probability density; and (4) binding sites are in equilibrium with Ca^{2+} ion concentration. Then conditioning on a configuration of Ca^{2+}

sources (RyRs and LCCs) reduced the FPE for individual ion locations and numbers to a reaction-diffusion equation (Tanskanen and Winslow, 2006). Since Ca^{2+} diffusion on nm length scales is several orders of magnitude faster than channel gating (an assumption also made by Hinch et al (2004; 2006)), Ca^{2+} ion density in the dyad equilibrates rapidly in each LCC and RyR gating state. This removed the time-dependence of the expected density of Ca^{2+} ions in the reaction-diffusion equation, yielding a Laplace equation, which under additional assumptions had an analytical solution for the spatial Ca^{2+} concentration profile (Tanskanen and Winslow, 2006). Thus, in general, the key to this multi-scale modeling approach was careful approximations regarding independence of Ca^{2+} ions (Debye length is short – under 1 nm) and successive rapid equilibrium approximations.

A more general issue, when model scalability is desired, is whether or not it is necessary to model the motion of individual signaling molecules in nano-domains, as in Tanskanen et al (2007). Under certain conditions, it is not necessary to do this, and use of reaction-diffusion equations for the spatio-temporal evolution of concentrations is appropriate. As shown elegantly by Tadross et al (2008) and Hake and Lines (2008), continuum approximations for stochastic molecular motions are appropriate when molecular flux within the nano-domain is large over the time-scale of changes in molecular conformations related to channel gating, binding of signaling molecules, or phosphorylation processes, as examples.

We believe that the examples offered above illustrate a common design motif in which proteins, protein complexes, and even organelles interact over short spatial and rapid time-scales to govern the processes of the cell. It is essential to continue efforts to understand the signal processing functions performed at these spatio-temporal scales, and to develop mathematically sound methods by which this information can be integrated to higher levels in order to understand the life of the cell.

Acknowledgments

Supported by National Institutes of Health grants HL081427, HL087345, HL105239, and HL1052160.

References

Ackerman MJ, Mohler PJ. Defining a new paradigm for human arrhythmia syndromes: phenotypic manifestations of gene mutations in ion channel- and transporter-associated proteins. Circ Res. 2010; 107:457–65. [PubMed: 20724725]

Ahrens-Nicklas RC, Clancy CE, Christini DJ. Re-evaluating the efficacy of β-adrenergic agonists and antagonists in long QT-3 syndrome through computational modelling. Cardiovascular Research. 2009; 82:439–447. [PubMed: 19264765]

Ai X, Curran JW, Shannon TR, Bers DM, Pogwizd SM. Ca2+/calmodulin-dependent protein kinase modulates cardiac ryanodine receptor phosphorylation and sarcoplasmic reticulum Ca2+ leak in heart failure. Circulation Research. 2005; 97:1314–22. [PubMed: 16269653]

Anderson ME, Mohler PJ. Rescuing a failing heart: think globally, treat locally. Nat Med. 2009; 15:25–6. [PubMed: 19129780]

Baddeley D, Jayasinghe ID, Lam L, Rossberger S, Cannell MB, Soeller C. Optical single-channel resolution imaging of the ryanodine receptor distribution in rat cardiac myocytes. Proc Natl Acad Sci U S A. 2009; 106:22275–80. [PubMed: 20018773]

Balaban RS. Cardiac energy metabolism homeostasis: Role of cytosolic calcium. Journal of Molecular and Cellular Cardiology. 2002; 34:1259–1271. [PubMed: 12392982]

Beard DA. A biophysical model of the mitochondrial respiratory system and oxidative phosphorylation. PLoS Comput Biol. 2005; 1:e36. [PubMed: 16163394]

Bers, DM. Excitation-Contraction Coupling and Cardiac Contractile Force. Kluwer; Boston: 2001.

Bers DM. Cardiac excitation-contraction coupling. Nature. 2002; 415:198–205. [PubMed: 11805843]

Bers DM. Calcium cycling and signaling in cardiac myocytes. Annu Rev Physiol. 2008; 70:23–49. [PubMed: 17988210]

Bers DM, Despa S. Na/K-ATPase--an integral player in the adrenergic fight-or-flight response. Trends Cardiovasc Med. 2009; 19:111–8. [PubMed: 19818946]

Bhalla US. Signaling in small subcellular volumes. I. Stochastic and diffusion effects on individual pathways. Biophysical Journal. 2004; 87:733–44. [PubMed: 15298882]

Bouchard RA, Clark RB, Giles WR. Role of sodium-calcium exchange in activation of contraction in rat ventricle. J Physiol. 1993; 472:391–413. [PubMed: 8145151]

Chance B, Williams GR. Method for the Localization of Sites for Oxidative Phosphorylation. Nature. 1955; 176:250–254. [PubMed: 13244669]

Cheng H, Lederer WJ, Cannell MB. Calcium sparks: elementary events underlying excitation-contraction coupling in heart muscle. Science. 1993; 262:740–4. [PubMed: 8235594]

Cooper J, Mirams GR, Niederer SA. High throughput functional curation of cellular electrophysiology models. Prog. Biophys. Mol. Biol. 2011; 105 note to publisher: please update before print.

Cortassa S, Aon MA, Marban E, Winslow RL, O'Rourke B. An integrated model of cardiac mitochondrial energy metabolism and calcium dynamics. Biophysical Journal. 2003; 84:2734–55. [PubMed: 12668482]

Cortassa S, Aon MA, O'Rourke B, Jacques R, Tseng HJ, Marban E, Winslow RL. A computational model integrating electrophysiology, contraction, and mitochondrial bioenergetics in the ventricular myocyte. Biophysical Journal. 2006; 91:1564–89. [PubMed: 16679365]

Cortassa S, O'Rourke B, Winslow RL, Aon MA. Control and regulation of mitochondrial energetics in an integrated model of cardiomyocyte function. Biophysical Journal. 2009; 96:2466–78. [PubMed: 19289071]

Csordas G, Renken C, Varnai P, Walter L, Weaver D, Buttle KF, Balla T, Mannella CA, Hajnoczky G. Structural and functional features and significance of the physical linkage between ER and mitochondria. Journal of Cell Biology. 2006; 174:915–921. [PubMed: 16982799]

Cunha SR, Bhasin N, Mohler PJ. Targeting and stability of Na/Ca exchanger 1 in cardiomyocytes requires direct interaction with the membrane adaptor ankyrin-B. Journal of Biological Chemistry. 2007; 282:4875–83. [PubMed: 17178715]

Cunha SR, Mohler PJ. Ankyrin protein networks in membrane formation and stabilization. J Cell Mol Med. 2009; 13:4364–76. [PubMed: 19840192]

Currie S, Loughrey CM, Craig MA, Smith GL. Calcium/calmodulin-dependent protein kinase IIdelta associates with the ryanodine receptor complex and regulates channel function in rabbit heart. Biochem J. 2004; 377:357–66. [PubMed: 14556649]

Dash RK, Qi F, Beard DA. A Biophysically Based Mathematical Model for the Kinetics of Mitochondrial Calcium Uniporter. Biophysical Journal. 2009; 96:1318–1332. [PubMed: 19217850]

Despa S, Tucker AL, Bers DM. Phospholemman-mediated activation of Na/K-ATPase limits [Na]i and inotropic state during beta-adrenergic stimulation in mouse ventricular myocytes. Circulation. 2008; 117:1849–55. [PubMed: 18362230]

Dick IE, Tadross MR, Liang H, Tay LH, Yang W, Yue DT. A modular switch for spatial Ca2+ selectivity in the calmodulin regulation of CaV channels. Nature. 2008; 451:830–4. [PubMed: 18235447]

El-Armouche A, Eschenhagen T. Beta-adrenergic stimulation and myocardial function in the failing heart. Heart Fail Rev. 2009; 14:225–41. [PubMed: 19110970]

Erickson MG, Alseikhan BA, Peterson BZ, Yue DT. Preassociation of calmodulin with voltage-gated Ca(2+) channels revealed by FRET in single living cells. Neuron. 2001; 31:973–85. [PubMed: 11580897]

Faber GM, Rudy Y. Action potential and contractility changes in [Na(+)](i) overloaded cardiac myocytes: a simulation study. Biophysical Journal. 2000; 78:2392–404. [PubMed: 10777735]

Franzini-Armstrong C, Protasi F, Ramesh V. Shape, size, and distribution of Ca(2+) release units and couplons in skeletal and cardiac muscles. Biophys J. 1999; 77:1528–39. [PubMed: 10465763]

Golovina VA, Song H, James PF, Lingrel JB, Blaustein MP. Na+ pump alpha(2)-subunit expression modulates Ca2+ signaling. American Journal of Physiology-Cell Physiology. 2003; 284:C475–C486. [PubMed: 12388076]

Grandi E, Puglisi JL, Wagner S, Maier LS, Severi S, Bers DM. Simulation of Ca-calmodulin-dependent protein kinase II on rabbit ventricular myocyte ion currents and action potentials. Biophysical Journal. 2007; 93:3835–47. [PubMed: 17704163]

Greenstein JL, Hinch R, Winslow RL. Mechanisms of excitation-contraction coupling in an integrative model of the cardiac ventricular myocyte. Biophys J. 2006; 90:77–91. [PubMed: 16214852]

Greenstein JL, Tanskanen AJ, Winslow RL. Modeling the actions of beta-adrenergic signaling on excitation--contraction coupling processes. Ann N Y Acad Sci. 2004; 1015:16–27. [PubMed: 15201146]

Greenstein JL, Winslow RL. An integrative model of the cardiac ventricular myocyte incorporating local control of Ca2+ release. Biophysical Journal. 2002; 83:2918–45. [PubMed: 12496068]

Hake J, Lines GT. Stochastic binding of Ca2+ ions in the dyadic cleft; continuous versus random walk description of diffusion. Biophys J. 2008; 94:4184–201. [PubMed: 18263662]

Hashambhoy YL, Greenstein JL, Winslow RL. Role of CaMKII in RyR leak, EC coupling and action potential duration: a computational model. J Mol Cell Cardiol. 2010; 49:617–24. [PubMed: 20655925]

Hashambhoy YL, Winslow RL, Greenstein JL. CaMKII-induced shift in modal gating explains L-type Ca(2+) current facilitation: a modeling study. Biophys J. 2009; 96:1770–85. [PubMed: 19254537]

Hayashi T, Martone ME, Yu Z, Thor A, Doi M, Holst MJ, Ellisman MH, Hoshijima M. Three-dimensional electron microscopy reveals new details of membrane systems for Ca2+ signaling in the heart. J Cell Sci. 2009; 122:1005–13. [PubMed: 19295127]

Hilgemann DW, Collins A, Matsuoka S. Steady-state and dynamic properties of cardiac sodium-calcium exchange. Secondary modulation by cytoplasmic calcium and ATP. J Gen Physiol. 1992; 100:933–61. [PubMed: 1484286]

Hinch R, Greenstein JL, Tanskanen AJ, Xu L, Winslow RL. A simplified local control model of calcium-induced calcium release in cardiac ventricular myocytes. Biophysical Journal. 2004; 87:3723–36. [PubMed: 15465866]

Hinch R, Greenstein JL, Winslow RL. Multi-scale models of local control of calcium induced calcium release. Prog Biophys Mol Biol. 2006; 90:136–50. [PubMed: 16321427]

Hudmon A, Schulman H, Kim J, Maltez JM, Tsien RW, Pitt GS. CaMKII tethers to L-type Ca2+ channels, establishing a local and dedicated integrator of Ca2+ signals for facilitation. Journal of Cell Biology. 2005; 171:537–47. [PubMed: 16275756]

Iancu RV, Jones SW, Harvey RD. Compartmentation of cAMP signaling in cardiac myocytes: a computational study. Biophys J. 2007; 92:3317–31. [PubMed: 17293406]

Jafri MS, Rice JJ, Winslow RL. Cardiac Ca2+ dynamics: the roles of ryanodine receptor adaptation and sarcoplasmic reticulum load. Biophysical Journal. 1998; 74:1149–68. [PubMed: 9512016]

Jayasinghe ID, Cannell MB, Soeller C. Organization of ryanodine receptors, transverse tubules, and sodium-calcium exchanger in rat myocytes. Biophys J. 2009; 97:2664–73. [PubMed: 19917219]

Katsnelson LB, Solovyova O, Balakin A, Lookin O, Konovalov P, Protsenko Y, Sulman T, Markhasin VS. Contribution of mechanical factors to arrhythmogenesis in calcium overloaded cardiomyocytes: Model predictions and experiments. Prog. Biophys. Mol. Biol. 2011; 105 note to publisher: please update before print.

Kizhatil K, Sandhu NK, Peachey NS, Bennett V. Ankyrin-B is required for coordinated expression of beta-2-spectrin, the Na/K-ATPase and the Na/Ca exchanger in the inner segment of rod photoreceptors. Exp Eye Res. 2009; 88:57–64. [PubMed: 19007774]

Kline CF, Cunha SR, Lowe JS, Hund TJ, Mohler PJ. Revisiting ankyrin-InsP(3) receptor interactions: Ankyrin-B associates with the cytoplasmic N-terminus of the InsP(3) receptor. Journal of Cellular Biochemistry. 2008; 104:1244–1253. [PubMed: 18275062]

Kuzumoto M, Takeuchi A, Nakai H, Oka C, Noma A, Matsuoka S. Simulation analysis of intracellular Na+ and Cl-homeostasis during beta 1-adrenergic stimulation of cardiac myocyte. Prog Biophys Mol Biol. 2008; 96:171–86. [PubMed: 17826821]

Langer GA, Peskoff A. Calcium concentration and movement in the diadic cleft space of the cardiac ventricular cell. Biophysical Journal. 1996; 70:1169–82. [PubMed: 8785276]

Larbig R, Torres N, Bridge JH, Goldhaber JI, Philipson KD. Activation of reverse Na+-Ca2+ exchange by the Na+ current augments the cardiac Ca2+ transient: evidence from NCX knockout mice. J Physiol. 2010; 588:3267–76. [PubMed: 20643777]

Litwin SE, Li J, Bridge JH. Na-Ca exchange and the trigger for sarcoplasmic reticulum Ca release: studies in adult rabbit ventricular myocytes. Biophys J. 1998; 75:359–71. [PubMed: 9649393]

Liu X, Spicarova Z, Rydholm S, Li J, Brismar H, Aperia A. Ankyrin B modulates the function of Na,K-ATPase/inositol 1,4,5-trisphosphate receptor signaling microdomain. Journal of Biological Chemistry. 2008; 283:11461–8. [PubMed: 18303017]

Lohn M, Furstenau M, Sagach V, Elger M, Schulze W, Luft FC, Haller H, Gollasch M. Ignition of calcium sparks in arterial and cardiac muscle through caveolae. Circ Res. 2000; 87:1034–9. [PubMed: 11090549]

Maack C, Cortassa S, Aon MA, Ganesan AN, Liu T, O'Rourke B. Elevated cytosolic Na+ decreases mitochondrial Ca2+ uptake during excitation-contraction coupling and impairs energetic adaptation in cardiac myocytes. Circ Res. 2006; 99:172–82. [PubMed: 16778127]

Maack C, O'rourke B. Excitation-contraction coupling and mitochondrial energetics. Basic Research in Cardiology. 2007; 102:369–392. [PubMed: 17657400]

Maier LS, Bers DM. Role of Ca2+/calmodulin-dependent protein kinase (CaMK) in excitation-contraction coupling in the heart. Cardiovascular Research. 2007; 73:631–40. [PubMed: 17157285]

Matsuoka S, Jo H, Sarai N, Noma A. An in silico study of energy metabolism in cardiac excitation-contraction coupling. Jpn J Physiol. 2004a; 54:517–22. [PubMed: 15760483]

Matsuoka S, Sarai N, Jo H, Noma A. Simulation of ATP metabolism in cardiac excitation-contraction coupling. Prog Biophys Mol Biol. 2004b; 85:279–99. [PubMed: 15142748]

Modchang C, Nadkarni S, Bartol TM, Triampo W, Sejnowski TJ, Levine H, Rappel WJ. A comparison of deterministic and stochastic simulations of neuronal vesicle release models. Phys Biol. 2010; 7:026008. [PubMed: 20505227]

Mohler PJ, Davis JQ, Bennett V. Ankyrin-B coordinates the Na/K ATPase, Na/Ca exchanger, and InsP3 receptor in a cardiac T-tubule/SR microdomain. PLoS Biol. 2005; 3:e423. [PubMed: 16292983]

Mohler PJ, Schott JJ, Gramolini AO, Dilly KW, Guatimosim S, duBell WH, Song LS, Haurogne K, Kyndt F, Ali ME, Rogers TB, Lederer WJ, Escande D, Le Marec H, Bennett V. Ankyrin-B mutation causes type 4 long-QT cardiac arrhythmia and sudden cardiac death. Nature. 2003; 421:634–9. [PubMed: 12571597]

Mohler PJ, Wehrens XH. Mechanisms of human arrhythmia syndromes: abnormal cardiac macromolecular interactions. Physiology (Bethesda). 2007; 22:342–50. [PubMed: 17928548]

Neco P, Rose B, Huynh N, Zhang R, Bridge JH, Philipson KD, Goldhaber JI. Sodium-calcium exchange is essential for effective triggering of calcium release in mouse heart. Biophys J. 2010; 99:755–64. [PubMed: 20682252]

Ostrom RS, Gregorian C, Drenan RM, Xiang Y, Regan JW, Insel PA. Receptor number and caveolar co-localization determine receptor coupling efficiency to adenylyl cyclase. J Biol Chem. 2001; 276:42063–9. [PubMed: 11533056]

Perkins GA, Renken CW, Frey TG, Ellisman MH. Membrane architecture of mitochondria in neurons of the central nervous system. Journal of Neuroscience Research. 2001; 66:857–865. [PubMed: 11746412]

Puglisi JL, Bers DM. LabHEART: an interactive computer model of rabbit ventricular myocyte ion channels and Ca transport. Am J Physiol Cell Physiol. 2001; 281:C2049–60. [PubMed: 11698264]

Risken, H. The Fokker-Planck equation. Springer; Berlin: 1997.

Rizzuto R, Pinton P, Carrington W, Fay FS, Fogarty KE, Lifshitz LM, Tuft RA, Pozzan T. Close contacts with the endoplasmic reticulum as determinants of mitochondrial Ca2+ responses. Science. 1998; 280:1763–1766. [PubMed: 9624056]

Rose WC, Balke CW, Wier WG, Marban E. Macroscopic and unitary properties of physiological ion flux through L-type Ca2+ channels in guinea-pig heart cells. J Physiol. 1992; 456:267–84. [PubMed: 1338098]

Rovetti R, Cui X, Garfinkel A, Weiss JN, Qu Z. Spark-induced sparks as a mechanism of intracellular calcium alternans in cardiac myocytes. Circulation Research. 2010; 106:1582–91. [PubMed: 20378857]

Ruehr ML, Russell MA, Bond M. A-kinase anchoring protein targeting of protein kinase A in the heart. J Mol Cell Cardiol. 2004; 37:653–65. [PubMed: 15350838]

Saucerman JJ, Bers DM. Calmodulin mediates differential sensitivity of CaMKII and calcineurin to local Ca2+ in cardiac myocytes. Biophysical Journal. 2008; 95:4597–612. [PubMed: 18689454]

Saucerman JJ, Brunton LL, Michailova AP, McCulloch AD. Modeling beta-adrenergic control of cardiac myocyte contractility in silico. Journal of Biological Chemistry. 2003; 278:47997–8003. [PubMed: 12972422]

Saucerman JJ, McCulloch AD. Cardiac beta-adrenergic signaling: from subcellular microdomains to heart failure. Ann N Y Acad Sci. 2006; 1080:348–61. [PubMed: 17132794]

Saucerman JJ, Zhang J, Martin JC, Peng LX, Stenbit AE, Tsien RY, McCulloch AD. Systems analysis of PKA-mediated phosphorylation gradients in live cardiac myocytes. Proc Natl Acad Sci U S A. 2006; 103:12923–8. [PubMed: 16905651]

Scarpa A, Graziotti P. Mechanisms for intracellular calcium regulation in heart. I. Stopped-flow measurements of Ca++ uptake by cardiac mitochondria. J Gen Physiol. 1973; 62:756–72. [PubMed: 4548716]

Scriven DR, Dan P, Moore ED. Distribution of proteins implicated in excitation-contraction coupling in rat ventricular myocytes. Biophys J. 2000; 79:2682–91. [PubMed: 11053140]

Sedova M, Dedkova EN, Blatter LA. Integration of rapid cytosolic Ca2+ signals by mitochondria in cat ventricular myocytes. American Journal of Physiology-Cell Physiology. 2006; 291:C840–C850. [PubMed: 16723510]

Serysheva II, Hamilton SL, Chiu W, Ludtke SJ. Structure of Ca2+ release channel at 14 A resolution. J Mol Biol. 2005; 345:427–31. [PubMed: 15581887]

Sham JS, Cleemann L, Morad M. Gating of the cardiac Ca2+ release channel: the role of Na+ current and Na(+)-Ca2+ exchange. Science. 1992; 255:850–3. [PubMed: 1311127]

Sham JS, Song LS, Chen Y, Deng LH, Stern MD, Lakatta EG, Cheng H. Termination of Ca2+ release by a local inactivation of ryanodine receptors in cardiac myocytes. Proc Natl Acad Sci U S A. 1998; 95:15096–101. [PubMed: 9844021]

Shannon TR, Ginsburg KS, Bers DM. Reverse mode of the sarcoplasmic reticulum calcium pump and load-dependent cytosolic calcium decline in voltage-clamped cardiac ventricular myocytes. Biophysical Journal. 2000; 78:322–33. [PubMed: 10620296]

Shannon TR, Wang F, Puglisi J, Weber C, Bers DM. A mathematical treatment of integrated Ca dynamics within the ventricular myocyte. Biophysical Journal. 2004; 87:3351–71. [PubMed: 15347581]

Sipido KR, Maes M, Van de Werf F. Low efficiency of Ca2+ entry through the Na(+)-Ca2+ exchanger as trigger for Ca2+ release from the sarcoplasmic reticulum. A comparison between L-type Ca2+ current and reverse-mode Na(+)-Ca2+ exchange. Circ Res. 1997; 81:1034–44. [PubMed: 9400385]

Sobie EA, Cannell MB, Bridge JH. Allosteric activation of Na+-Ca2+ exchange by L-type Ca2+ current augments the trigger flux for SR Ca2+ release in ventricular myocytes. Biophys J. 2008; 94:L54–6. [PubMed: 18223001]

Soeller C, Cannell MB. Numerical simulation of local calcium movements during L-type calcium channel gating in the cardiac diad. Bipphys. J. 1997; 73:97–111.

Soeller C, Cannell MB. Analysing cardiac excitation-contraction coupling with mathematical models of local control. Progress in Biophysics & Molecular Biology. 2004; 85:141–162. [PubMed: 15142741]

Song LS, Wang SQ, Xiao RP, Spurgeon H, Lakatta EG, Cheng H. beta-Adrenergic stimulation synchronizes intracellular Ca(2+) release during excitation-contraction coupling in cardiac myocytes. Circulation Research. 2001; 88:794–801. [PubMed: 11325871]

Sosinsky GE, Deerinck TJ, Greco R, Buitenhuys CH, Bartol TM, Ellisman MH. Development of a model for microphysiological simulations: small nodes of ranvier from peripheral nerves of mice reconstructed by electron tomography. Neuroinformatics. 2005; 3:133–62. [PubMed: 15988042]

Stern MD. Theory of excitation-contraction coupling in cardiac muscle. Biophysical Journal. 1992; 63:497–517. [PubMed: 1330031]

Stern MD, Song LS, Cheng H, Sham JS, Yang HT, Boheler KR, Rios E. Local control models of cardiac excitation-contraction coupling. A possible role for allosteric interactions between ryanodine receptors. J Gen Physiol. 1999; 113:469–89. [PubMed: 10051521]

Su Z, Sugishita K, Ritter M, Li F, Spitzer KW, Barry WH. The sodium pump modulates the influence of I-Na on [Ca2+](i) transients in mouse ventricular myocytes. Biophysical Journal. 2001; 80:1230–1237. [PubMed: 11222287]

Swift F, Tovsrud N, Enger UH, Sjaastad I, Sejersted OM. The Na+/K+-ATPase alpha2-isoform regulates cardiac contractility in rat cardiomyocytes. Cardiovascular Research. 2007; 75:109–17. [PubMed: 17442282]

Tadross MR, Dick IE, Yue DT. Mechanism of local and global Ca2+ sensing by calmodulin in complex with a Ca2+ channel. Cell. 2008; 133:1228–40. [PubMed: 18585356]

Tanskanen A, Winslow RL. Integrative, structurally-detailed model of calcium dynamics in the cardiac diad. SIAM Journal of Multiscale Modeling and Simulation. 2006; 5:1280–1296.

Tanskanen AJ, Greenstein JL, Chen A, Sun SX, Winslow RL. Protein geometry and placement in the cardiac dyad influence macroscopic properties of calcium-induced calcium release. Biophys J. 2007; 92:3379–96. [PubMed: 17325016]

Tanskanen AJ, Greenstein JL, O'Rourke B, Winslow RL. The role of stochastic and modal gating of cardiac L-type Ca2+ channels on early after-depolarizations. Biophysical Journal. 2005; 88:85–95. [PubMed: 15501946]

Terracciano CM. Rapid inhibition of the Na+-K+ pump affects Na+-Ca2+ exchanger-mediated relaxation in rabbit ventricular myocytes. J Physiol. 2001; 533:165–73.a. [PubMed: 11351025]

Territo PR, French SA, Dunleavy MC, Evans FJ, Balaban RS. Calcium activation of heart mitochondrial oxidative phosphorylation - Rapid kinetics of m(V) over dot (O2), NADH, and light scattering. Journal of Biological Chemistry. 2001; 276:2586–2599. [PubMed: 11029457]

Thomas MJ, Sjaastad I, Andersen K, Helm PJ, Wasserstrom JA, Sejersted OM, Ottersen OP. Localization and function of the Na+/Ca2+-exchanger in normal and detubulated rat cardiomyocytes. J Mol Cell Cardiol. 2003; 35:1325–37. [PubMed: 14596789]

Wang H, Peskin CS, Elston TC. A robust numerical algorithm for studying biomolecular transport processes. J. Theor. Biol. 2003; 221

Wang MC, Collins RF, Ford RC, Berrow NS, Dolphin AC, Kitmitto A. The three-dimensional structure of the cardiac L-type voltage-gated calcium channel: comparison with the skeletal muscle form reveals a common architectural motif. J. Biol. Chem. 2004a; 279:7159–68. [PubMed: 14634003]

Wang SQ, Stern MD, Rios E, Cheng H. The quantal nature of Ca2+ sparks and in situ operation of the ryanodine receptor array in cardiac cells. Proc Natl Acad Sci U S A. 2004b; 101:3979–84. [PubMed: 15004280]

Wasserstrom JA, Vites AM. The role of Na(+)-Ca2+ exchange in activation of excitation-contraction coupling in rat ventricular myocytes. J Physiol. 1996; 493(Pt 2):529–42. [PubMed: 8782114]

Wilson MA, Brunger AT. the 1.0 A crystal structure of Ca2+-bound calcmodulin: an analysis of disorder and implications for functionally relevant plasticity. J. Mol. Biol. 2000; 301(5):1237–1256. [PubMed: 10966818]

Yang JH, Saucerman JJ. Computational models reduce complexity and accelerate insight into cardiac signaling networks. Circ Res. 2011; 108:85–97. [PubMed: 21212391]

Yang Z, Pascarel C, Steele DS, Komukai K, Brette F, Orchard CH. Na+-Ca2+ exchange activity is localized in the T-tubules of rat ventricular myocytes. Circ Res. 2002; 91:315–22. [PubMed: 12193464]

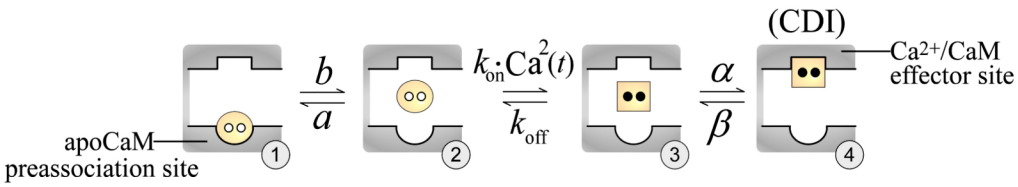

Figure 1.

Basic states for a lobe of CaM in complex with a Ca^{2+} channel (from (Tadross et al., 2008)). In state 1, apoCaM (yellow circle) is bound to the apoCaM site (round pocket). In state 2, apoCaM is a transiently dissociated. In state 3, CaM binds two Ca^{2+} ions (black dots) to become Ca^{2+}/CaM (yellow square), which can then bind the Ca^{2+}/CaM effector site (square pocket), yielding CDI (state 4).

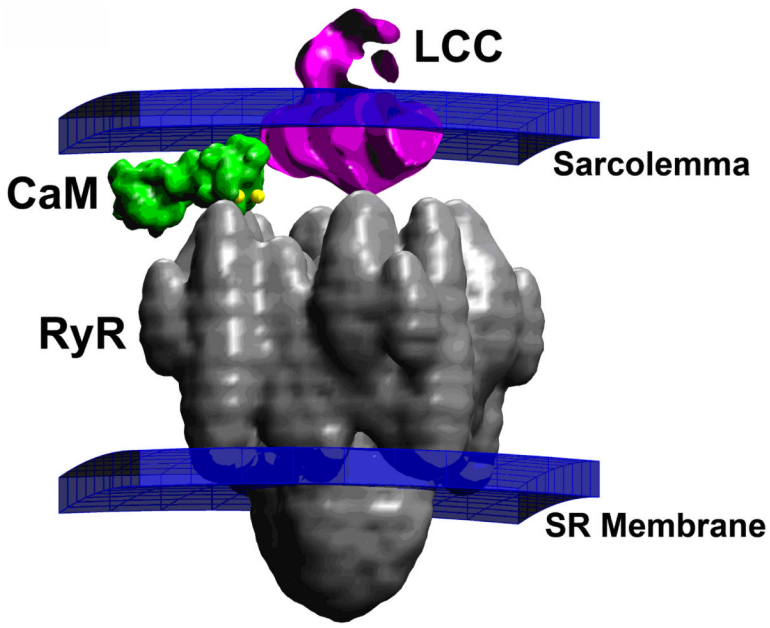

Figure 2.
Structure of a region of the dyad containing one LCC opposed to a single RyR, and one CaM molecule tethered to the LCC (Tanskanen et al., 2007).

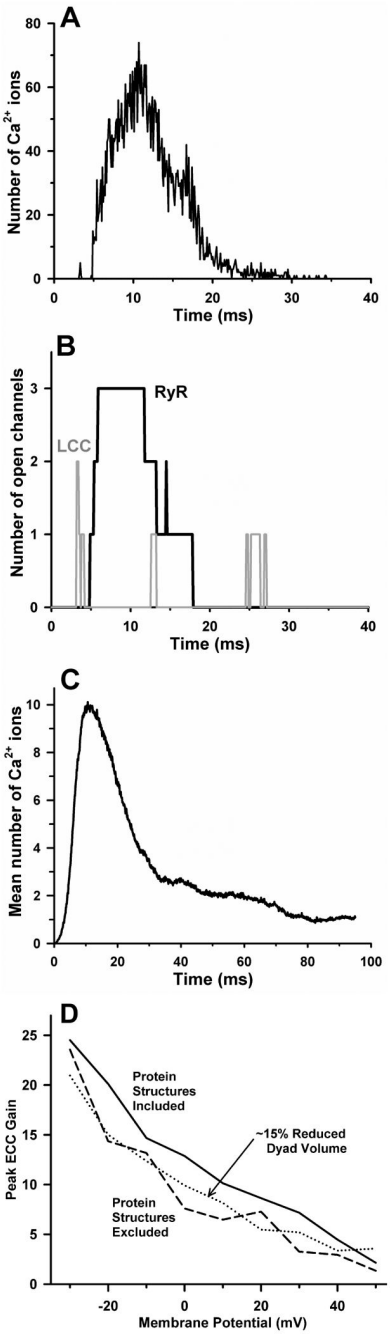

Figure 3.

A CICR event in a single dyad evoked by a 0 mV voltage clamp step at time zero (from (Tanskanen et al., 2007)). (A) The number of free Ca^{2+} ions in the dyad volume as a function of time. (B) The number of open RyRs (black solid line) and the number of open LCCs (gray solid line) in the dyad during the release event depicted in panel A. (C) The average number of free Ca^{2+} ions in the dyad as calculated from 1000 independent dyads. (D) ECC gain (averaged over 400 independent dyad simulations) as a function of membrane potential for the baseline model which includes space-filling geometric models of protein structure in the dyad (solid line), for the model with protein structures excluded (dashed

line), and for a modified model with dyad height reduced from 15 nm to 13 nm and protein structures excluded (dotted line).

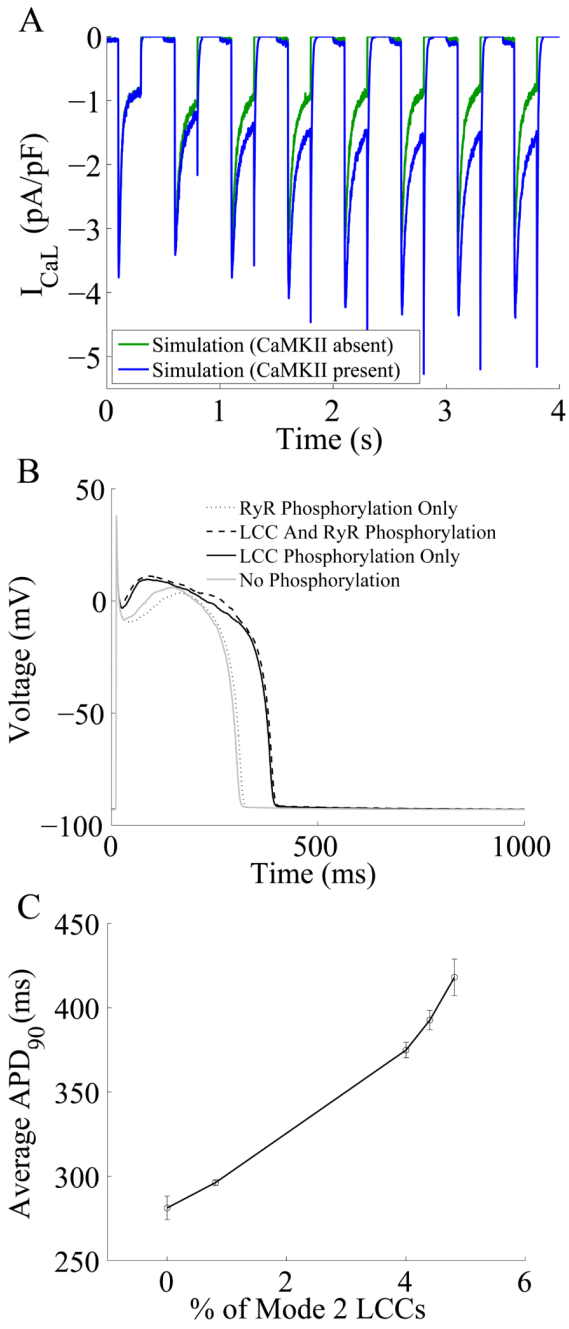

Figure 4.

(A) Simulated I_{CaL} elicited by a rapid pacing protocol in which a prepulse of −40 mV was delivered, followed by a 200 ms depolarization to 0mV (from (Hashambhoy et al., 2009)). Holding potential was −80 mV. Blue curves represent model results in the presence of CaMKII and green curves represent model results in the absence of CaMKII. (B) Simulated Results from a 1-Hz AP pacing protocol under different LCC and/or RyR phosphorylation conditions. (C) AP duration as a function of average LCC phosphorylation levels. Fully phosphorylated LCCs gate in Mode 2 which exhibit long duration openings (Hashambhoy et al., 2010).

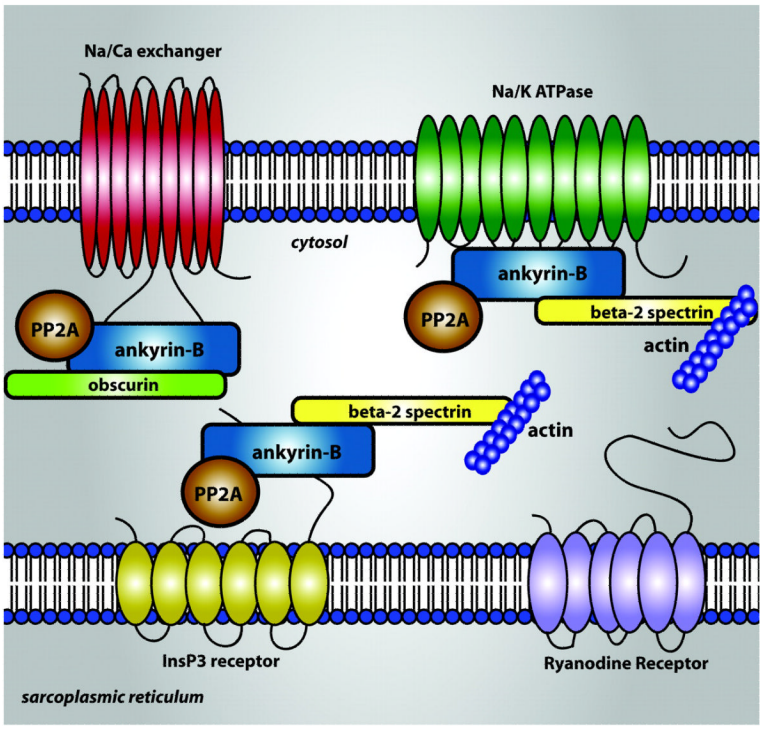

Figure 5.
Schematic illustration of ANK-B binding to and co-localization of NCX, NKA, and $InsP_3R$. ANK-B also binds the actin associated β2-spectrin, the cytoskeletal protein obscurin, and the regulatory sub-unit of protein phosphatase (PP) 2A (Ackerman and Mohler, 2010).